4-18-2017

^{1}H NMR Shows Slow Phospholipid Flip-Flop in Gel and Fluid Bilayers

Drew Marquardt
Universitat Graz

Frederick A. Heberle
The University of Tennessee, Knoxville

Tatiana Miti
University of South Florida, Tampa

Barbara Eicher
Universitat Graz

Erwin London
Stony Brook University

See next page for additional authors

LANGMUIR

Article

pubs.acs.org/Langmuir

^{1}H NMR Shows Slow Phospholipid Flip-Flop in Gel and Fluid Bilayers

Drew Marquardt,[*,†,‡,◆] Frederick A. Heberle,[*,§,∥,⊥,◆] Tatiana Miti,[#] Barbara Eicher,[†,‡] Erwin London,[¶] John Katsaras,[§,⊥,▽,○] and Georg Pabst[*,†,‡]

[†]Institute of Molecular Biosciences, Biophysics Division, NAWI Graz, University of Graz, Graz 8010, Austria

[‡]BioTechMed-Graz, Graz 8010, Austria

[§]The Bredesen Center and [○]Department of Physics and Astronomy, University of Tennessee, Knoxville, Tennessee 37996, United States

[∥]Joint Institute for Biological Sciences, [⊥]Biology and Soft Matter Division, and [▽]Shull Wollan Center—A Joint Institute for Neutron Sciences, Oak Ridge National Laboratory, Oak Ridge, Tennessee 37831, United States

[#]Department of Physics, University of South Florida, Tampa, Florida 33620, United States

[¶]Department of Biochemistry and Cell Biology, Stony Brook, New York 11794, United States

Supporting Information

ABSTRACT: We measured the transbilayer diffusion of 1,2-dipalmitoyl-*sn*-glycero-3-phosphocholine (DPPC) in large unilamellar vesicles, in both the gel ($L_{\beta'}$) and fluid (L_α) phases. The choline resonance of headgroup-protiated DPPC exchanged into the outer leaflet of headgroup-deuterated DPPC-*d*13 vesicles was monitored using ^{1}H NMR spectroscopy, coupled with the addition of a paramagnetic shift reagent. This allowed us to distinguish between the inner and outer bilayer leaflet of DPPC, to determine the flip-flop rate as a function of temperature. Flip-flop of fluid-phase DPPC exhibited Arrhenius kinetics, from which we determined an activation energy of 122 kJ mol^{-1}. In gel-phase DPPC vesicles, flip-flop was not observed over the course of 250 h. Our findings are in contrast to previous studies of solid-supported bilayers, where the reported DPPC translocation rates are at least several orders of magnitude faster than those in vesicles at corresponding temperatures. We reconcile these differences by proposing a defect-mediated acceleration of lipid translocation in supported bilayers, where long-lived, submicron-sized holes resulting from incomplete surface coverage are the sites of rapid transbilayer movement.

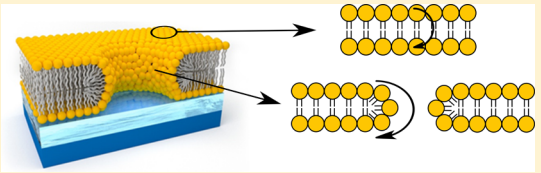

INTRODUCTION

The eukaryotic plasma membrane (PM) is characterized by an asymmetric distribution of lipids between the exoplasmic and cytoplasmic bilayer leaflets.[1−3] The physiological fate of cells depends on the strict maintenance of this asymmetry through the interplay of active and passive lipid translocation events.[4] Active mechanisms are thought to rely on the so-called floppases that move newly synthesized lipids from the inner to the outer leaflet and on flippases that restore the asymmetry of passively translocated lipids.[5,6] The selectivity of these enzymes for different classes of lipids regulates compositional asymmetry within the PM.[4] For example, the exoplasmic leaflet of mammalian PM is enriched with sphingolipids and neutral phosphatidylcholines, whereas the cytoplasmic leaflet contains most of the aminophospholipids, including phosphatidylethanolamines and negatively charged phosphatidylserines.[7] Still, the exact mechanisms by which these lipids arrive and remain at their locations in the PM are not fully understood.[8] Reliable values of passive lipid translocation rates are a necessary starting point for a detailed mechanistic understanding of PM asymmetry, but such values are both scarce and scattered, with reported flip-flop half times for PC lipids in the fluid phase ranging from minutes[9] to hours[10] to days or weeks.[11−13] Even less is known about flip-flop kinetics of lipids in the highly ordered gel state.[14−17] The frequent use of extrinsic probe molecules has undoubtedly contributed to the controversy surrounding spontaneous lipid translocation.

Model phospholipid bilayers have long served as surrogates for the systematic and well-controlled investigation of biological membrane phenomena. A variety of sample geometries have been developed, including freely floating liposomes and solid-supported bilayers (SSBs).[18] Different sample geometries have associated advantages and disadvantages and are often chosen out of necessity for a particular experiment. For example, recent studies have utilized SSBs for measuring passive lipid translocation with sum-frequency generation (SFG) vibrational spectroscopy.[14−17] In these studies, SSBs were chosen for the facile preparation of asymmetric bilayers as well as because of the surface-sensitive nature of the measurement technique. Inherent differences between SSBs and vesicles—most notably, the close proximity of the support to the membrane and the presence of edges and defects in SSBs—raise the possibility of differences in lipid translocation behavior.[19] Recent developments in the methodology for preparing and characterizing

Received: December 14, 2016
Revised: January 19, 2017
Published: January 20, 2017

DOI: 10.1021/acs.langmuir.6b04485
Langmuir 2017, 33, 3731−3741

asymmetric vesicles[20] now allow for a comparison of lipid translocation in bilayers having different sample geometries without the need for bulky labels, which may not faithfully report on the behavior of the host lipid.[14]

Making use of these developments, we report on the passive lipid transbilayer diffusion of the gel ($L_{\beta'}$) and fluid (L_α) phase 1,2-dipalmitoyl-*sn*-glycero-3-phosphocholine (DPPC) in tensionless, probe-free liposomes.[20] Use of asymmetric vesicles having different DPPC isotopes in the inner and outer leaflets enabled measurement of intrinsic flip-flop rates using solution ^{1}H NMR. We find that DPPC flip-flop in the gel phase is too slow to accurately measure, whereas fluid-phase DPPC undergoes flip-flop with a temperature-dependent half time ranging from days to weeks. Vesicles incubated within the main transition at 40 °C exhibited approximately a twofold faster flip-flop rate than fully melted fluid vesicles at 50 °C. At all temperatures we examined, the translocation rate in vesicles is slower by orders of magnitude than that previously measured with SFG on supported DPPC bilayers.[14,16] We propose a plausible defect-mediated mechanism, supported by Monte Carlo simulations, to explain the dramatic acceleration of lipid translocation in supported bilayers compared to vesicles.

RESULTS

Structure of Asymmetric DPPC Vesicles. We make use of asymmetric large unilamellar vesicles (aLUVs) to measure lipid translocation. To this end, aLUVs of DPPC and its deuterated variants (Figure S1) were prepared by cyclodextrin-mediated lipid exchange as previously described.[20] We exchanged headgroup-protiated/chain-perdeuterated donor lipid (DPPC-*d*C) into LUVs initially composed of headgroup-deuterated/chain-protiated acceptor lipid (DPPC-*d*H). The use of differentially deuterated donor and acceptor lipids allowed us to determine the composition of each leaflet after exchange using isotope-sensitive techniques, namely, ^{1}H NMR combined with gas chromatography (GC), as previously described.[20] On average, aLUVs had an outer leaflet donor concentration of 59 mol % (i.e., 59% of outer leaflet acceptor lipid was replaced by donor lipid) and an inner leaflet donor concentration of 30 mol % immediately following exchange. The appearance of inner leaflet donor lipid may result from a small population of otherwise undetectable donor vesicle contamination or from accelerated flip-flop during the exchange step when vesicles are subjected to a relatively high cyclodextrin concentration.[21] However, neither of these cases affects the analysis or interpretation of kinetic data presented below.

Because bilayer defects can promote lipid translocation,[8] vesicle structure was assessed before and after lipid exchange. Vesicle size and polydispersity were measured using dynamic light scattering (DLS), and the bilayer structure was determined from SAXS measurements. SAXS is particularly useful as these measurements probe the internal bilayer structure, which can be compared to that of symmetric LUVs prepared using conventional methods. Figure 1 shows experimental SAXS form factors, $\mathrm{FF}(q) = q \times \mathrm{sgn}[I(q)]\sqrt{|I(q)|}$, for symmetric and asymmetric DPPC vesicles. Within experimental uncertainty, these form factors are identical. Bilayer structural parameters were obtained by fitting the form factors to a slab model, as described previously[22] and are listed in Table 1. The area per lipid (A_L), headgroup−headgroup spacing (D_{HH}), and hydrocarbon thickness ($2D_C$) are similar for symmetric and asymmetric vesicles and compare well to the literature values. Furthermore, vesicle size and polydispersity measured using DLS were similar before and after the lipid exchange (Figure 1c) and did not change significantly during sample incubation (Figure 1d). Together, these results indicate that the asymmetric vesicle preparation did not introduce structural artifacts. A similar conclusion was drawn in a previous study that compared symmetric and asymmetric LUVs composed of 1-palmitoyl-2-oleoyl-*sn*-glycero-3-phosphocholine (POPC) and its deuterated analogs and which used the same asymmetric vesicle preparation method.[20]

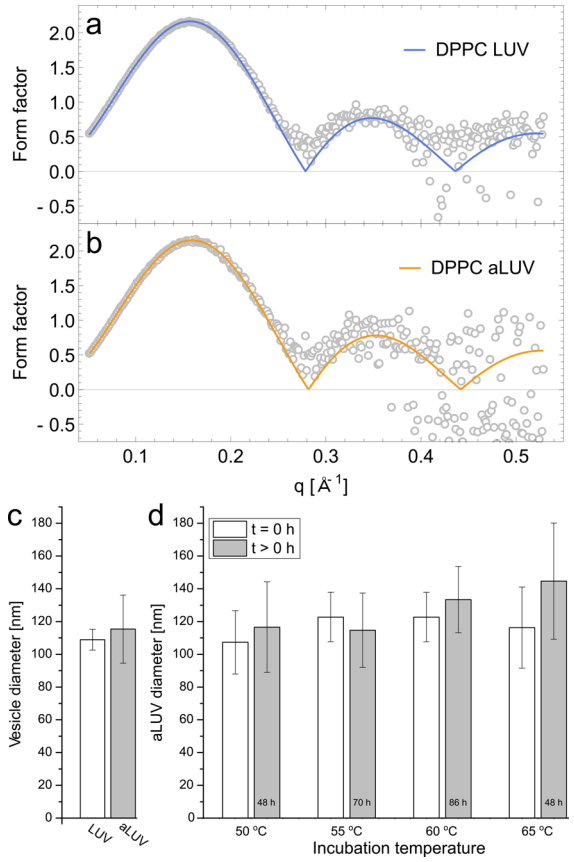

Figure 1. Structure of symmetric and asymmetric DPPC vesicles. Experimental small-angle X-ray scattering (SAXS) form factors (open circles) and fits (solid colored lines) for DPPC LUVs prepared using standard extrusion (a) and aLUVs (DPPC-*d*H^{inner}/DPPC-*d*C^{outer}) prepared by cyclodextrin-mediated exchange (b), both at 55 °C. (c) Vesicle diameter of acceptor LUVs (white bars) and aLUVs (solid bars) immediately after preparation. (d) aLUV diameter before (white bars) and after (solid bars) incubation at different temperatures (incubation times are indicated on the bars).

Table 1. DPPC Structural Parameters Obtained from Refinement of SAXS Data[a,b]

	LUV	aLUV	literature[c]
A_L (Å^2)	65.7	65.7	64.05
D_{HH} (Å)	35.2	34.8	36.55
$2D_C$ (Å)	27.5	27.5	28.18

[a]Best fit parameters for extruded symmetric and asymmetric DPPC bilayers (LUV and aLUV, respectively) at 55 °C: area per lipid (A_L), headgroup−headgroup distance (D_{HH}), and hydrocarbon thickness ($2D_C$). [b]Parameter uncertainty is estimated to be ±2%. [c]Data from Kučerka et al.[23]

DOI: 10.1021/acs.langmuir.6b04485
Langmuir 2017, 33, 3731−3741

Thermotropic Behavior of Asymmetric DPPC Vesicles. We used differential scanning calorimetry (DSC) to compare the thermotropic behavior of symmetric and asymmetric DPPC vesicles in D_2O. Figure 2 shows exotherms for vesicles composed of DPPC and its isotopic variants. Protiated DPPC multilamellar vesicles (MLVs) (Figure 2, upper) exhibited a broad $L_{\beta'} \rightarrow P_{\beta'}$ pretransition (T_P) centered at 35.5 °C and a relatively narrow $P_{\beta'} \rightarrow L_\alpha$ main transition (T_M) centered at 42.0 °C, consistent with previous reports.[24] Deuteration of the PC headgroup resulted in only a slight decrease in T_P and T_M (<1 °C), whereas chain perdeueration resulted in a larger decrease of 3−4 °C, also in agreement with the literature.[25] These results, summarized in Table S1, are consistent with hydrocarbon chain melting as the dominant contribution to the transitions.

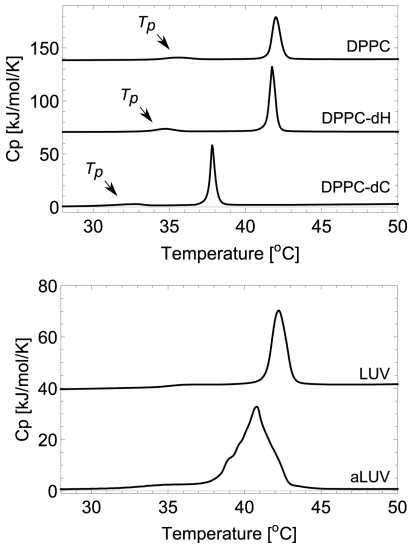

Figure 2. Differential scanning calorimetry of DPPC vesicles in D_2O. Upper: exotherms of DPPC MLVs composed of different isotopic variants. Lower: exotherms for DPPC LUVs and DPPC-dH^{in}/DPPCdC^{out} aLUVs. Data were collected at a scan rate of 0.5 °C/s.

Extrusion to form symmetric 100 nm LUVs caused a broadening of the phase transitions (Figure 2, lower), as observed previously.[26] In aLUVs with a DPPC-dH-enriched inner leaflet and a DPPC-dC-enriched outer leaflet, an even broader transition that includes multiple peaks was apparent; indeed, the aLUV exotherm is well-fit by a sum of a single broad Gaussian representing the pretransition and three Gaussians representing the main transition (Figure S2 and Table S2). It was previously found that in homogeneous mixtures of protiated and chain-perdeuterated DPPC, T_M shifted linearly as a function of mixture composition and was only slightly broadened.[27] The presence of two main transition peaks is therefore an expected outcome from aLUVs having two weakly coupled leaflets of different isotopic compositions. The additional complexity of the aLUV thermogram may indicate sample heterogeneity, including heterogeneous exchange and/or minor contamination from symmetric donor or

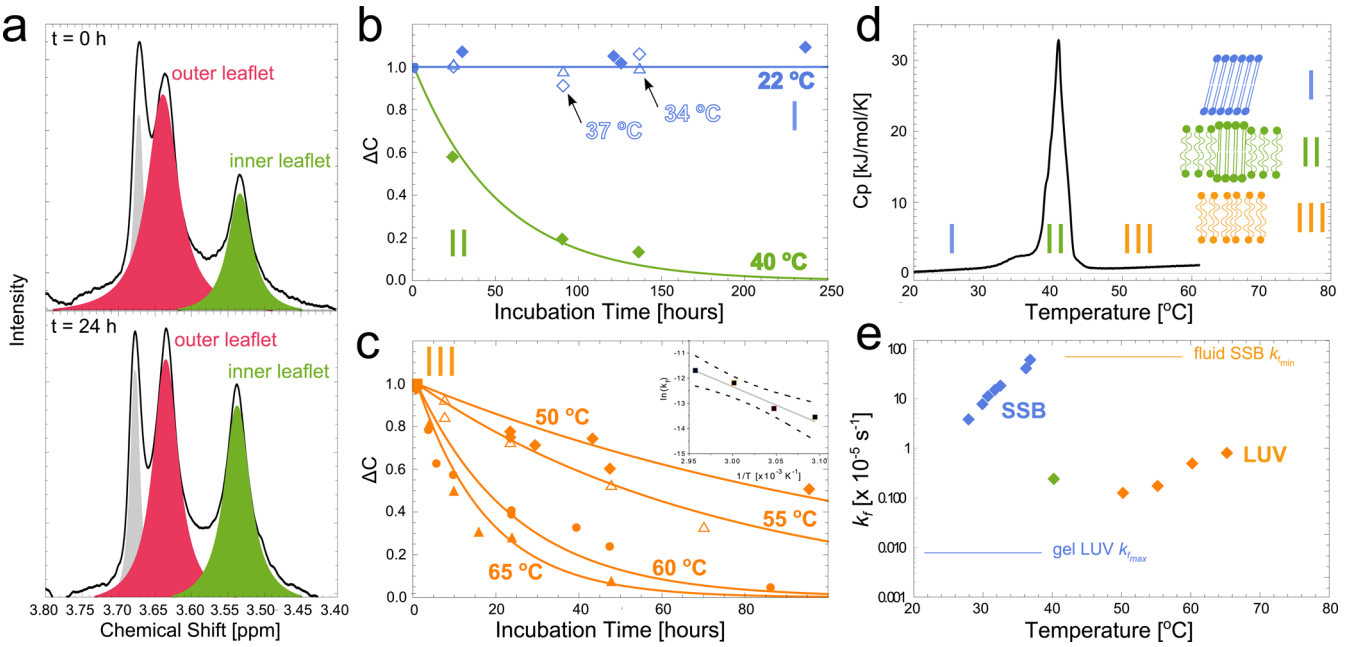

Figure 3. DPPC flip-flop kinetics. (a) Asymmetric lipid distribution determined by ^{1}H NMR. Shown are NMR data (black line) and fitted components (filled peaks) from DPPC-dH^{in}/DPPC-dC^{out} aLUVs in the presence of ∼70 μM Pr^{3+} shift reagent, measured immediately following aLUV preparation (upper panel) and after 24 h incubation at 65 °C (lower panel). Spectra were modeled as the sum of outer leaflet (red) and inner leaflet (green) choline resonances and residual aqueous cyclodextrin (gray). (b,c) Time decay of normalized bilayer asymmetry at various temperatures in the gel (blue symbols), gel + fluid (green symbols), and fluid (orange symbols) phases and fits to eq 3 (solid lines). ΔC is defined as the difference in inner and outer leaflet NMR peak areas normalized to their initial (time zero) difference, see eq 3. Inset to (c) shows the Arrhenius behavior of fluid-phase translocation (solid gray line, with dashed lines indicating the 95% confidence interval). (d) DSC exotherm for DPPC-dH^{in}/DPPCdC^{out} aLUVs. Roman numerals denote different bilayer phase states and are color-coded to the data in (b) and (c): I, gel (blue); II, gel + fluid coexistence (green); and III, fluid (orange). (e) Translocation rate constants (k_f) for gel phase (blue, SSB values reproduced from Liu and Conboy),[14] gel + fluid coexistence (green), and fluid-phase (orange) DPPC. Horizontal lines represent the minimum k_f for SSB fluid-phase DPPC and the maximum gel-phase k_f for LUVs.

DOI: 10.1021/acs.langmuir.6b04485
Langmuir 2017, 33, 3731−3741

acceptor vesicles. Alternatively, it may reflect stronger coupling of the asymmetric leaflets. Importantly, the kinetic analysis presented below is not influenced by the presence of symmetric vesicle contamination.

Interestingly, both LUV exotherms clearly showed the presence of a ripple phase. The ripple phase has previously been observed experimentally in both unilamellar vesicles[28−31] and in symmetric single SSBs.[32,33] However, the cooperativity of lipid phase transitions is much higher in multibilayer stacks due to the confinement of out-of-plane fluctuations[30] and is a likely reason for the failure to detect the $L_{\beta'} \rightarrow P_{\beta'}$ transition in some reports of unilamellar systems.[34,35] On the basis of the DSC data in Figure 2, it is clear that gel-phase flip-flop measurements should be made below 30 °C to avoid the ripple phase, especially when deuterated lipids are used.

Translocation of DPPC in Gel- and Fluid-Phase Vesicles. Asymmetric lipid distributions in aLUVs were quantified from solution ^{1}H NMR spectra measured in the presence of extravesicular paramagnetic lanthanide ions Pr^{3+}.[36] aLUVs were prepared and incubated at a desired temperature in the absence of Pr^{3+}, and at regular time intervals, a sample aliquot was removed to quantify the asymmetry, with Pr^{3+} added immediately before the NMR measurement. Externally added Pr^{3+} (~70 μM) does not permeate into the vesicle lumen during the ~15 min NMR measurement,[20,36] interacting only with outer leaflet lipid headgroups and inducing a downfield shift of the DPPC choline resonance (we note that the deuterated choline of DPPC-*d*H does not contribute to the ^{1}H NMR signal). The observed choline signal is therefore a superposition of shifted and unshifted resonances with relative areas that are proportional to the amount of DPPC in the outer and inner leaflets, respectively (Figure 3a).[36]

Freshly prepared aLUVs whose outer leaflets were initially enriched in headgroup-protiated DPPC (i.e., DPPC-dH^{in}/DPPCdC^{out}) exhibited an unequal area ratio that gradually approached unity as lipids equilibrated between the two bilayer leaflets (Figure 3a, lower panel). The normalized temperature- and time-dependent transbilayer lipid distributions obtained from NMR are shown in Figure 3b,c. We determined the flip-flop rate constant k_f at different temperatures directly from changes in the asymmetric lipid distribution as a function of time. Fitted decay curves for fluid-phase DPPC are shown in Figure 3c. In the temperature range of 50−65 °C, we observed flip-flop rates ranging from 1.3×10^{-6} to 8.3×10^{-6} s^{-1}, corresponding to flip-flop half-times ($t_{1/2}$) on the order of days to weeks (Table 2).

We further investigated DPPC flip-flop in the gel phase (22, 34, and 37 °C) and within the main phase transition at 40 °C (Figure 3d). We did not observe appreciable flip-flop of gel-phase DPPC for incubation times up to 250 h. However, when LUVs were incubated within the main transition at 40 °C, the flip-flop rate was a factor of 2 greater than that measured for fully melted fluid DPPC at 50 °C and a factor of 5 greater than that expected from an extrapolation of higher-temperature data. Flip-flop rate constants (k_f) and half-times ($t_{1/2}$) for DPPC at various temperatures are summarized in Table 2.

From the temperature dependence of k_f (Figure 3c, inset), we found that the kinetics for fluid-phase DPPC flip-flop follow Arrhenius' law. The activation energy barrier for flip-flop was determined by fitting to the Arrhenius equation, $k_f = A \exp(-E_a/RT)$, yielding $E_a = 122 \pm 14$ kJ/mol. Additional thermodynamic parameters were determined using transition state theory.[13] These values are summarized in Table S3.

Table 2. Summary of DPPC Translocation Kinetics

temperature (°C)	phase	k_f ($\times 10^{-6}$ s^{-1})	$t_{1/2}$ (h)
20	$L_{\beta'}$	<0.085[a]	>4555[a]
34			
37			
40	$P_{\beta'} + L_\alpha$	2.5 ± 0.2	75 ± 6
50	L_α	1.3 ± 0.08	147 ± 9
55		1.8 ± 0.09	105 ± 5
60		5.1 ± 0.5	38 ± 3
65		8.3 ± 0.4	23 ± 1

[a]No flip-flop was observed in gel-phase vesicles.

Simulations of Defect-Mediated Translocation. As speculated previously[19] and confirmed in this work, liposomes exhibit remarkably different flip-flop behavior than supported bilayers. One contributing factor might be submicron topological defects that are known to exist in SSBs from atomic force microscopy (AFM) imaging studies.[33,37−46] To investigate the influence of defects on flip-flop, we performed random-walk (Monte Carlo) simulations of lateral lipid diffusion in the presence of 100 nm-diameter holes, a typical size observed in AFM images.[46] Figure 4a shows a schematic illustration of such a defect (not to scale) in a supported bilayer. We assumed that translocation effectively occurs by unhindered lateral diffusion of a lipid through the pore formed by the lipid headgroups. Flip-flop was therefore incorporated into the simulations by enforcing a translocation event whenever a proposed random step carried a lipid into a hole (full details of the simulations are found in the Experimenal Procedures).

Figure 4b shows a typical simulated lipid trajectory, characterized by relatively long time periods during which a lipid meandered through the space between holes, before finally approaching a hole edge. This was followed by a series of alternating flip and flop events as the lipid diffused in the vicinity of the hole edge; for the particular trajectory shown in Figure 4b, 47 separate translocation events occurred. Eventually, the lipid wandered away from the hole to repeat the cycle. The outcome of this sequence of events is effectively a randomization of the lipid's transbilayer location.

Simulations were performed at three values of bilayer surface coverage, 99.0, 99.5, and 99.9% (Figure 4c), using diffusion coefficients typical of gel-phase DPPC (10^{-4} to 10^{-2} μm^2 s^{-1}).[32] We observed asymmetry decay curves (Figure 4d, open symbols) similar to those measured using SFG for gel-phase DPPC in supported bilayers.[14] These curves were well fit by a double exponential decay (Figure 4d, solid lines), and the range of obtained values for the slower component k_f (Figure 4e) was consistent with reported rates for gel-phase translocation in SSBs.[14] As expected, either increasing the diffusion coefficient or decreasing the surface coverage (i.e., increasing the defect density) increased the translocation rate (Figure 4e). Furthermore, a fluid-phase diffusion coefficient of 1 μm^2 s^{-1} (equivalent to compressing the time axis of Figure 4d by a factor of 10^3) resulted in complete equilibration of the two leaflets within seconds, even for 99.9% surface coverage. This observation is consistent with reports that SSBs prepared by Langmuir−Blodgett/Langmuir−Schaefer (LB/LS) deposition do not support asymmetry at fluid-phase temperatures.[14] We conclude that defect-mediated translocation is a plausible mechanism to reconcile the observed differences between vesicles and SSBs.

DOI: 10.1021/acs.langmuir.6b04485
Langmuir 2017, 33, 3731−3741

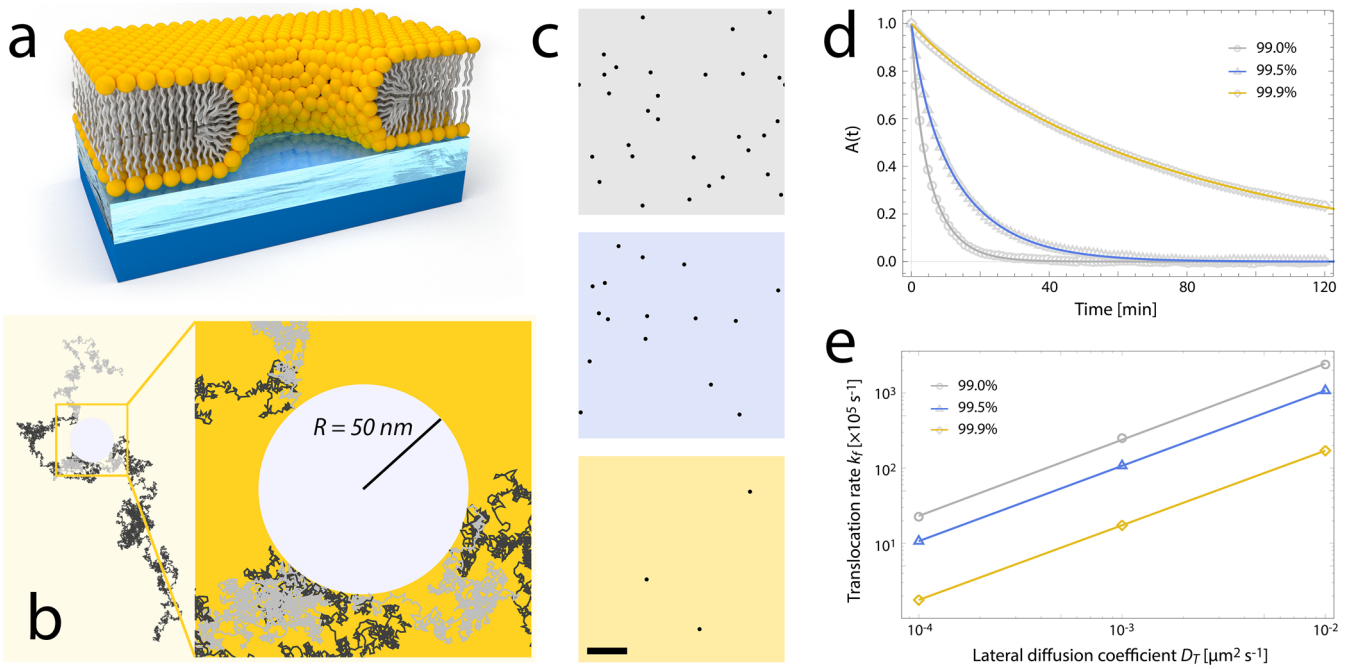

Figure 4. Monte Carlo simulations of defect-mediated flip-flop. (a) Schematic illustration of an SSB, showing a defect site in cross-section. Transbilayer movement is assumed to occur via unhindered lateral diffusion through the pore formed by lipid headgroups. (b) MC simulation snapshot of a particle trajectory that includes segments in the top (black) and bottom (gray) leaflets. The inset shows an expanded view in the vicinity of a circular defect, revealing multiple translocation events. (c) Top−down view of simulation snapshots (defects shown as black circles; scale bar, 1 μm) for different bilayer surface coverages: 99.0% (gray), 99.5% (blue) and 99.9% (yellow). (d) Simulated asymmetry decay curves (open symbols) and fits (solid lines) corresponding to the surface coverages in (c), for a lateral lipid diffusion coefficient of 10^{-3} μm^2 s^{-1}. (e) Lipid translocation rate k_f vs lateral diffusion coefficient D_T calculated from decay curves corresponding to the surface coverages in (c).

DISCUSSION

We measured flip-flop kinetics in vesicles using ^{1}H NMR by following the transbilayer movement of a headgroup-protiated lipid in a headgroup-deuterated matrix. DPPC in the fluid phase showed the expected increase in k_f (decrease in $t_{1/2}$) with increasing temperature (Figure 3c,e and Table 2). Still, DPPC flip-flop is slow, even at fluid-phase temperatures; for example, a half time of nearly 6 days was found at 50 °C. Slow translocation is nevertheless consistent with many previous reports for PC lipids in vesicles,[13,20,47−49] including the inability of a SANS study to detect intrinsic POPC flip-flop at 37 °C over a period of 2 days.[21] A significant advantage of our method is the ability to measure the intrinsic flip-flop rate of the host lipid (here, DPPC) as opposed to that of an extrinsic probe molecule. For example, Homan and Pownall found a fourfold increase in flip-flop half time of a prenyl phospholipid in a host POPC vesicle when the probe chain length was varied from 8 to 12 carbons.[13]

Translocation in Vesicles is Dramatically Slower than that in SSBs. Our observation of slow DPPC translocation in vesicles stands in contrast to previously published gel-phase DPPC flip-flop rates in SSBs measured using SFG,[14,17] a method that also measures intrinsic lipid translocation and is therefore directly comparable to the present work. Indeed, our data suggest that accurate flip-flop measurements may not even be possible for gel-phase lipids in vesicles because of the extremely slow kinetics of flip-flop when compared with the vesicle lifetime.

That flip-flop rates measured in vesicles and SSBs are different, is perhaps unsurprising.[19] Membrane properties including lateral diffusion[50,51] and phase behavior[52,53] are known to exhibit a complex dependence on the properties of the support as well as the bilayer deposition technique.[54,55] The sheer variety of SSB systems—including different substrates, cushions, tethers, and deposition techniques—precludes a simple explanation of their flip-flop behavior. For example, Tamm and co-workers have successfully retained asymmetry for hours in fluid-phase SSBs prepared using the Langmuir−Blodgett/vesicle fusion (LB/VF) technique.[54,55] We therefore restrict the following discussion to supported bilayers prepared using LB/LS deposition onto uncushioned quartz substrates, for which extensive flip-flop data exist.[14,17] Below, we discuss three possible explanations for the differences in flip-flop rates in this system compared with vesicles: these include the phase state of the sample, the presence of bilayer curvature in vesicles, and the presence of topological bilayer defects such as edges and pores in SSBs.

Translocation is Accelerated in Phase Coexistence Regions. We found that DPPC flip-flop in vesicles is accelerated when the sample is incubated within the main phase transition, an effect that was previously reported for a fluorescent nitrobenzoxadiazole-labeled lipid (C6-NBD-PC) in host DPPC vesicles.[9] Bilayer permeability reaches a maximum in the vicinity of the main transition,[56] where enhanced area fluctuations lead to a greater probability of spontaneous pore formation.[57] The interface of gel/fluid domain boundaries may be particularly leaky.[58] One possible explanation for accelerated flip-flop in SSBs is therefore the presence of a broadened gel + fluid coexistence region (33−41.5 °C) in supported DPPC bilayers, as shown by Wu and co-workers using SFG and AFM.[46] Other SFG studies have also found a similarly broad main phase transition for DPPC SSBs.[59] Although published values for DPPC flip-flop rates measured in the temperature range 27.7−36.6 °C were all ascribed to the gel phase,[14] it is

DOI: 10.1021/acs.langmuir.6b04485
Langmuir 2017, 33, 3731−3741

possible that at least some of these rates were actually measured within the gel + fluid coexistence region and would therefore be expected to have enhanced translocation. Nevertheless, our observations in vesicles suggest that this would result in at most a factor of five increase in the translocation rate, which cannot fully account for the orders-of-magnitude discrepancy between vesicles and SSBs.

Influence of Vesicle Curvature. Although we did not directly address the influence of curvature on flip-flop rate in the present study, two lines of evidence suggest that bilayer curvature effects should be minimal for the 100 nm-diameter DPPC vesicles used in our NMR measurements. First, for a wide variety of neutral PC lipids, X-ray scattering data obtained from flat oriented bilayer stacks and extruded LUVs (50 nm pore size) are in excellent agreement over a large q range, suggesting a negligible influence of curvature on the bilayer structure.[23,60,61] Moreover, these data were well-fit by a symmetric bilayer form factor, implying an identical structure for the inner and outer leaflets. (A caveat is that vesicle curvature may have a more pronounced effect on the structure of bilayers composed of charged lipids, as observed by Brustowicz and Brunger for SOPS vesicles[62] and Kučerka and co-workers for DOPS vesicles,[61] although this finding is not relevant to our experiments on zwitterionic PC lipids.) Second, it was previously reported that lipid asymmetry is stable for days in a variety of systems having vastly different vesicle curvature, namely, SUVs of <30 nm diameter,[47] LUVs of ∼50−150 nm diameter,[63,64] and GUVs of >20 micron diameter.[49,65] This finding suggests that flip-flop rate is not strongly dependent upon curvature, and more importantly that the slow flip-flop reported here for 100 nm-diameter DPPC LUVs is not an artifact of vesicle curvature.

Topological Defects in Solid-Supported Bilayers. The topology of a sealed vesicle is fundamentally different from that of a supported bilayer. In the former, the outer and inner leaflets are distinct surfaces, whereas in the latter the two leaflets are continuous, meeting at the macroscopic edges of the substrate and at any defect sites, as shown schematically in Figure 4a. In an SSB, lipids can therefore move from the proximal to the distal leaflet (and vice versa) effectively by lateral diffusion through a permanent or defect edge. Although the permanent substrate edge is an unavoidable consequence of the sample geometry, it is likely not a significant contributor to translocation for centimeter-sized substrates, as most lipids would need to diffuse long distances to reach the nearest edge. On the other hand, AFM images of SSB generally show numerous patches of bare substrates appearing as holes with submicron dimensions (tens to hundreds of nanometers in diameter); these are especially ubiquitous in gel-phase bilayers.[33,37−46] Moreover, for typical values of bilayer surface coverage, the average distance between holes is on the order of microns or less.[46] Although these defects are often too small to be seen with conventional fluorescence microscopy, they can be detected with other fluorescence techniques. For example, in LB/LS supported bilayers containing fluorescent NBD-labeled lipids in both leaflets, external addition of the reducing agent dithionite—which does not permeate intact bilayers[66]—nevertheless quenched the fluorescence on both sides of the supported bilayer, implying the existence of numerous small defects in SSB that could not otherwise be visualized with fluorescence microscopy.[54] These defects are apparently long-lived and are most likely due to incomplete coverage and lipid contraction and desorption during the bilayer deposition process.[40]

Translocation is Accelerated by Defects. MC simulations revealed dramatically accelerated translocation in bilayers containing even a low density of defects (Figure 4c−e). The translocation rate exhibited a linear dependence on the lateral diffusion coefficient (D_T), increasing by 2 orders of magnitude with a 100-fold increase in D_T, which may help explain the observed strong dependence of flip-flop rate on temperature in gel-phase SSBs.[14] Using supported bilayers, Tamm and McConnell found that the lateral diffusion coefficient of gel-phase DPPC increased from 10^{-4} μm^2 s^{-1} at room temperature to 10^{-2} μm^2 s^{-1} at the pretransition, with an associated activation energy of 400 kJ mol^{-1} (compared with ∼40 kJ mol^{-1} for fluid-phase diffusion).[32] The authors attributed this unusually large activation energy to a defect-mediated diffusion process in the gel phase. Given the strong temperature dependence of D_T in the gel phase, any process that is limited by translational diffusion would also be expected to exhibit a strong temperature dependence. A second factor that influences translocation kinetics in our simulations is defect density, but this parameter has not been systematically explored experimentally. Typical reported values of surface coverage are >95%, but these may also depend on temperature.[67]

Our simulations, while highly simplified, nevertheless indicate that a better understanding of lateral diffusion is needed to explain translocation in supported bilayers. There are three potentially distinct environments in an SSB—the distal leaflet, the proximal leaflet, and the defect edge—and therefore at least three diffusion rates to consider. For example, there is evidence to suggest that lateral diffusion may be slower in the proximal leaflet compared to the distal leaflet.[50] Much less is known about the nature of the bilayer in the vicinity of a defect. Molecular dynamics (MD) simulations suggest that lipids located within a defect are more disordered and that lipid movement through the edge may actually be *faster* than lateral diffusion in the bulk.[68] Experimental studies of mechanically stressed vesicles also indicate that translocation is accelerated by the presence of defects.[69] The implication of these findings is that in a bilayer with a sufficient density of long-lived defects, the translocation rate will be controlled by the time that it takes for a lipid to diffuse to the nearest defect and not by the actual translocation event at the defect edge itself. Indeed, an MD simulation of pore-mediated flip-flop found that after spontaneous formation of a small water channel in the bilayer, the majority of ensuing flip-flop events were for lipids that were initially remote from the pore but that diffused to the pore site with time.[70] Still, other experimental studies have found increased order and reduced mobility of fluorescent lipid probes located near the edges of nanopatterned supported bilayers,[71] suggesting the existence of an energy barrier for a lipid to enter or leave the edge region that might slow translocation. More experimental and simulation work is needed to understand the nature of the defect edge environment and how it contributes to flip-flop rates in supported bilayers.

Influence of Pr^{3+} on Translocation Measurements. In the current study, samples were incubated in the absence of Pr^{3+}, which was introduced immediately before NMR measurements. We demonstrated in previous work that Pr^{3+} does not cross the bilayer on the time scale of our NMR measurements, even upon temperature cycling through T_M.[20] Previous studies have shown an increase in T_M with increasing Pr^{3+}

DOI: 10.1021/acs.langmuir.6b04485
Langmuir 2017, 33, 3731−3741

concentration.[72−74] We also observe a concentration-dependent increase in T_M of DPPC due to Pr^{3+} (Figure S3). However, for conditions within the NMR sample tube (~70 μM Pr^{3+}, 75:1 lipid/Pr^{3+}), there is only a minor increase in T_M, such that aLUVs were fully melted at the measurement temperature of 50 °C. Furthermore, after the addition of Pr^{3+} to the sample, successively recorded NMR spectra were identical (Figure S4), indicating that Pr^{3+} does not measureably accelerate flip-flop during the data collection interval. We therefore conclude that Pr^{3+} reports faithfully on flip-flop rates and does not itself influence the transbilayer distribution of lipids.

SUMMARY AND CONCLUSIONS

We used NMR to determine passive lipid flip-flop rates in asymmetric vesicles composed of DPPC and its deuterated variants. This novel experimental approach allowed us to avoid complications associated with bulky fluorescence or spin labels. We were unable to observe flip-flop in gel-phase vesicles over the course of weeks. Even at elevated temperatures, fluid-phase DPPC exhibited relatively slow flip-flop, with half times ranging from ~1 week at 50 °C to ~1 day at 65 °C. From the observed Arrhenius behavior, we determined the activation free energy, enthalpy, and entropy of DPPC translocation in vesicles.

We found significant differences in flip-flop rates of lipids in vesicles compared with the literature data from supported bilayers. Specifically, DPPC flip-flop in SSBs prepared by LB/LS[14] deposition is at least several orders-of-magnitude faster than that in LUVs at the same temperature. The ubiquity of submicron holes in SSBs seen with AFM imaging suggests that these differences are most likely due to the different nature of bilayer defects in these systems. This conclusion is supported by MC simulations, which show rapid equilibration of the proximal and distal leaflets (seconds to hours) in the presence of holes, even for gel-phase diffusion and what would be considered excellent surface coverages. We are not the first to urge caution when equating the behaviors of model systems having different sample geometries,[75] let alone when extrapolating these results to biological membranes,[76,77] which do not fit neatly into simple categories.

Despite these caveats, we do not wish to imply that SSBs have no value for translocation studies. On the contrary, SSBs may provide a more realistic model for cellular membranes that are often supported by a cytoskeleton. SSBs are also potentially a powerful platform for systematic investigation of defect-mediated translocation. In addition to facile access to translocation rates through SFG measurements, the use of SSBs enables direct visualization of even submicron defects with AFM, allowing for a thorough characterization of defect size and lifetime distributions. Such information will likely be crucial for modeling translocation. Moreover, it may be possible to control defect characteristics by using micro- or nano-patterned substrates. There has long been speculation that *all* lipid translocation is fundamentally a defect-mediated process,[78] irrespective of the sample geometry, owing to the prohibitively large energetic cost of desolvating the polar headgroup.[79] In recent years, MD simulations have lent support to this idea.[80,81] Because supported bilayers potentially offer greater control over defect characteristics, SSB-based translocation studies may ultimately shed new light on this long-standing problem in membrane biophysics.

EXPERIMENTAL PROCEDURES

Materials. 1,2-Dipalmitoyl-*sn*-glycero-3-phosphocholine (16:0/16:0 PC, DPPC), 1,2-dipalmitoyl-*d*62-*sn*-glycero-3-phosphocholine [16:0(*d*31)/16:0(*d*31) PC, DPPC-*d*C], 1,2-dipalmitoyl-*sn*-glycero-3-phosphocholine-1,1,2,2-d4-*N*,*N*,*N*-trimethyl-*d*9 [16:0/16:0 PC(*d*13), DPPC-*d*H], and 1,2-dipalmitoyl-*sn*-glycero-3-phospho-(1′-*rac*-glycerol) (sodium salt) [16:0/16:0 PG, DPPG] were purchased from Avanti Polar Lipids (Alabaster, AL) and used as received. Lipid stock solutions were prepared by dissolving dry lipid powder in HPLC-grade chloroform. Methyl-β-cyclodextrin (mβCD) was purchased from Acros Organics (Thermo Fisher Scientific, Waltham, MA) and prepared as a 35 mM stock solution in H_2O. Praseodymium(III) nitrate hexahydrate $Pr(NO_3)_3{\cdot}6H_2O$ (Pr^{3+}) was purchased from Alfa Aesar (Ward Hill, MA) and prepared as a 100 mM stock solution in D_2O. Centrifugal filter devices (Amicon Ultra-15, 100 000 Da molecular weight cutoff) were purchased from EMD Millipore (Billerica, MA) and washed seven times with H_2O before use to remove trace glycerol. Ultrapure H_2O was obtained from a High-Q purification system (Wilmette, IL), and 99.9% D_2O was purchased from Cambridge Isotopes (Andover, MA).

Preparation of aLUVs. We prepared aLUVs from DPPC and its deuterated headgroup (DPPC-*d*H) and acyl chain (DPPC-*d*C) variants using cyclodextrin-mediated lipid exchange, described in detail elsewhere.[20,82] Briefly, extruded 100 nm-diameter acceptor LUVs (10−12 mg/mL) provided lipids for the aLUV inner leaflet, whereas donor MLVs provided different lipids for the outer leaflet. An excess of donor lipid (threefold over acceptor) was used. Donor MLVs were prepared in a 20% (w/w) sucrose solution to increase their density and facilitate their separation from aLUVs following the exchange step, in which donor and acceptor vesicles were gently stirred for 1 h at room temperature in the presence of 30 mM mβCD. The mixture was then diluted eightfold with H_2O and centrifuged at 20 000 × *g* for 30 min to pellet donor MLVs. The supernatant containing aLUVs was concentrated using a prewashed 100 kDa molecular weight cutoff centrifugal filtration device at 5000 × *g*. Three subsequent cycles of dilution with D_2O and concentration in the centrifugal filter allowed the efficient removal of residual sucrose and mβCD as well as exchange of H_2O with D_2O for NMR measurements.

Characterization of aLUVs. Samples for SAXS were concentrated to 20 mg/mL and measured with a Rigaku BioSAXS-2000 home source system with a Pilatus 100K detector and a HF007 copper rotating anode (Rigaku Americas, The Woodlands, TX). SAXS data were collected at a fixed sample-to-detector distance using a silver behenate calibration standard. Samples for 90° DLS were diluted to ~60 μM and measured with a Brookhaven BI-200SM system (Brookhaven Instruments, Holtsville, NY). Samples for DSC were measured at ~5 mg/mL using a Nano DSC (TA Instruments, New Castle, DE). Sample composition was determined with GC using procedures outlined by Heberle et al.[20] Analysis was performed on an Agilent 5890A gas chromatograph (Santa Clara, CA) with a 5975C mass-sensitive detector operated in the electron-impact mode. An HP-5MS capillary column (30 m × 0.25 mm, 0.25 μm film thickness) was used with a helium carrier at 1 mL/min and an inlet temperature of 270 °C.

Translocation Measurements with ^{1}H NMR. Lipid translocation rates were determined from proton nuclear magnetic resonance (^{1}H NMR) spectroscopic measurements. Isotopically asymmetric aLUVs were prepared, and an aliquot was immediately measured using the shift reagent technique described below to establish a time zero (t = 0) data point. Vesicles were incubated at 22, 34, 37, 40, 50, 55, 60, and 65 °C, with aliquots removed at regular time intervals for measurement. Separate sample preparations were used to populate different temperature data to minimize preparation-specific bias.

^{1}H NMR spectra were collected on an Avance III 400 MHz spectrometer using the Bruker TopSpin acquisition software and analyzed with TopSpin 3.2. Lipid suspensions in D_2O were brought to a total volume of 0.6 mL (for a total lipid concentration of ~5 mM) and loaded into 5 mm NMR tubes. A standard ^{1}H pulse sequence with a 30° flip angle and 2 s delay time was employed to collect 1664

DOI: 10.1021/acs.langmuir.6b04485
Langmuir 2017, 33, 3731−3741

transients at 50 °C. Data were processed with a line-broadening parameter of 2 Hz. The distribution of protiated choline between inner and outer vesicle leaflets was determined by the addition of the shift reagent Pr^{3+}. Briefly, immediately before measurement, 2 μL of 20 mM Pr^{3+}/D_2O solution was dispensed directly into the NMR tube, which was then capped and inverted a minimum of three times to mix the contents. Several Pr^{3+} additions were made, with spectra obtained between between titrations, and the sample was discarded after measurement. The choline resonance was modeled using one or two Lorentzian peaks in the absence or presence of Pr^{3+}, respectively. Spectra obtained from 2−3 successive Pr^{3+} additions were modeled separately to determine the inner and outer leaflet area fractions.

Kinetic Model for Lipid Translocation. In general, an analysis of vesicle exchange kinetics must consider both intervesicle and intravesicle (flip-flop) contributions to the decay of signals. For example, Nakano and co-workers were able to determine both inter- and intravesicle exchange rates in a time-resolved SANS experiment by mixing two populations of initially symmetric LUVs (one protiated and one deuterated).[21] However, owing to our initial conditions (i.e., a single population of identical aLUVs), vesicle−vesicle exchange does not contribute to the observed kinetics. This allowed us to determine the flip-flop rate constant k_f directly from changes in the asymmetric lipid distribution as a function of time.

Asymmetry decay curves were modeled by solving a first-order, homogeneous system of equations that accounts for both inter- and intravesicle lipid transport (a complete derivation is found in the Supporting Information). Briefly, the inner and outer leaflet peak areas obtained from ^{1}H NMR are proportional to the inner and outer leaflet concentrations of choline-protiated lipid C_{in} and C_{out}, given by

$$C_{in}(t) = \frac{1}{2}\left[1 + \frac{C_{in}(0) - C_{out}(0)}{C_{in}(0) + C_{out}(0)}\, e^{-2k_f t}\right] \quad (1)$$

$$C_{out}(t) = \frac{1}{2}\left[1 - \frac{C_{in}(0) - C_{out}(0)}{C_{in}(0) + C_{out}(0)}\, e^{-2k_f t}\right] \quad (2)$$

Taking the difference in peak areas and normalizing to their initial difference gives the decay curve

$$\Delta C(t) \equiv \frac{C_{out}(t) - C_{in}(t)}{C_{out}(0) - C_{in}(0)} = e^{-2k_f t} \quad (3)$$

The translocation half time is found by setting eq 3 equal to 0.5 and solving for t, yielding

$$t_{1/2} = \frac{\ln(2)}{2k_f} \quad (4)$$

Measurements at multiple temperatures allowed the determination of the activation energy E_a, using the Arrhenius equation

$$k_f = A\, e^{-E_a/RT} \quad (5)$$

where R is the universal gas constant and A is the pre-exponential factor. Other thermodynamic quantities including the enthalpy and entropy of formation of the activated state ($\Delta H^{\ddagger}$ and $\Delta S^{\ddagger}$, respectively) and the free energy of activation $\Delta G^{\ddagger}$ were calculated using transition state theory following Homan and Pownall.[13]

Monte Carlo Simulations of Defect-Mediated Translocation. Simulations of 2D lipid diffusion in the presence of defects were performed using custom code written in Mathematica 11.0 (Wolfram Research, Champaign, IL). Particle trajectories were generated by first choosing a random initial particle position (x_0, y_0) within a periodic box of side length l (representing a square patch of bilayer) and assigning the particle to the top or bottom leaflet. During each uniform time step τ, the particle was advanced a uniform distance δ in a random direction within its leaflet, specified by an angle θ drawn from a uniform probability distribution $\theta \sim U(0, 2\pi)$. Particle trajectories generated in this way satisfy the probability distribution for a 2D random walk

$$p(x, y, t|x_0, y_0) = \frac{1}{4\pi D t} \exp\left[-\frac{(x - x_0)^2 + (y - y_0)^2}{4Dt}\right] \quad (6)$$

where the diffusion coefficient $D = \delta^2/4\tau$.

To simulate defect-mediated translocation, nonoverlapping circular holes of radius R were randomly placed within the simulation box. The number of holes N_H in a given box was drawn from a Poisson distribution $N_H \sim \text{Poisson}(\lambda)$, where λ is the mean number of holes, given by

$$\lambda = \frac{l^2(1 - \sigma)}{\pi R^2} \quad (7)$$

and σ is the fractional bilayer surface coverage (e.g., 0.99). Because holes represent bare substrate, particles were not allowed to occupy a position within a hole. The following rule was therefore applied to each proposed distance step: if the step carried the particle into a hole, the particle maintained its previous (x, y) position but was reassigned to the opposite leaflet, a movement that corresponds to translocation via lateral diffusion through the hole edge. To minimize the unphysical possibility of a particle "jumping" over a hole in a single step, the distance step was chosen such that $\delta < 0.1R$.

To relate an ensemble of particle trajectories to asymmetry decay curves, each particle was initially and arbitrarily assigned a random position within the top leaflet. The fractional asymmetry parameter A was then calculated as

$$A(t) = \frac{N_{P,top}(t) - N_{P,bot}(t)}{N_P} \quad (8)$$

where N_P was the total number of simulated particles, and $N_{P,top}$ and $N_{P,bot}$ were the number of particles in the top and bottom leaflets, respectively. For the asymmetry decay curves presented in Figure 4d, a total of 10^4 particle trajectories were simulated in 10 boxes of side length l = 50 μm, each having a different random configuration of holes. The resulting decay curves were averaged and fit to a double exponential decay,

$$A(t) = A_1\, e^{-k_1 t} + (1 - A_1)\, e^{-k_2 t} \quad (9)$$

with the slower decay component reported as the flip-flop rate constant k_f in Figure 4e.

■ ASSOCIATED CONTENT

Supporting Information

The Supporting Information is available free of charge on the ACS Publications website at DOI: 10.1021/acs.langmuir.6b04485.

Chemical structures of DPPC and its deuterated variants, DPPC thermodynamic parameters obtained from fitting DSC data, DSC thermograms for DPPC in the presence of Pr^{3+}, of Pr 3+, thermodynamic parameters determined from the temperature dependence of DPPC translocation, and a detailed derivation of a kinetic flip-flop (PDF)

■ AUTHOR INFORMATION

Corresponding Authors

*E-mail: marquardtdt@ornl.gov (D.M.).
*E-mail: heberlefa@ornl.gov (F.A.H.).
*E-mail: georg.pabst@uni-graz.at (G.P.).

ORCID

Drew Marquardt: 0000-0001-6848-2497
Georg Pabst: 0000-0003-1967-1536

Author Contributions

◆D.M. and F.A.H. contributed equally.

DOI: 10.1021/acs.langmuir.6b04485
Langmuir 2017, 33, 3731−3741

Notes

The authors declare no competing financial interest.

■ ACKNOWLEDGMENTS

The authors thank Santa Jansone-Popova for NMR technical assistance. This work acknowledges support from the Austrian Science Fund (FWF) project P27083 (to G.P.); the University of Tennessee−Oak Ridge National Laboratory (ORNL) Joint Institute for Biological Sciences (to F.A.H.); the National Science Foundation (NSF) DMR 1404985 (to E.L.); and the Laboratory Directed Research and Development Program award 7394 (to J.K. and F.A.H.) from ORNL, managed by UT-Battelle, LLC, under US Department of Energy (DOE) contract no. DE-AC05-00OR22725. SAXS, DLS, and DSC measurements were supported by DOE scientific user facilities.

■ REFERENCES

(1) Bretscher, M. S. Asymmetrical Lipid Bilayer Structure for Biological Membranes. *Nature, New Biol.* **1972**, *236*, 11−12.
(2) Bretscher, M. S. Membrane Structure: Some General Principles. *Science* **1973**, *181*, 622−629.
(3) Op den Kamp, J. A. F. Lipid Asymmetry in Membranes. *Annu. Rev. Biochem.* **1979**, *48*, 47−71.
(4) Daleke, D. L. Regulation of transbilayer plasma membrane phospholipid asymmetry. *J. Lipid Res.* **2003**, *44*, 233−242.
(5) Devaux, P. F. Protein involvement in transmembrane lipid asymmetry. *Annu. Rev. Biophys. Biomol. Struct.* **1992**, *21*, 417−439.
(6) Serra, M. V.; Kamp, D.; Haest, C. W. M. Pathways for flip-flop of mono- and di-anionic phospholipids in the erythrocyte membrane. *Biochim. Biophys. Acta, Biomembr.* **1996**, *1282*, 263−273.
(7) van Meer, G.; Voelker, D. R.; Feigenson, G. W. Membrane lipids: Where they are and how they behave. *Nat. Rev. Mol. Cell Biol.* **2008**, *9*, 112−124.
(8) Contreras, F.-X.; Sánchez-Magraner, L.; Alonso, A.; Goñi, F. M. Transbilayer (flip-flop) lipid motion and lipid scrambling in membranes. *FEBS Lett.* **2010**, *584*, 1779−1786.
(9) John, K.; Schreiber, S.; Kubelt, J.; Herrmann, A.; Müller, P. Transbilayer Movement of Phospholipids at the Main Phase Transition of Lipid Membranes: Implications for Rapid Flip-Flop in Biological Membranes. *Biophys. J.* **2002**, *83*, 3315−3323.
(10) Kornberg, R. D.; McConnell, H. M. Inside-outside transitions of phospholipids in vesicle membranes. *Biochemistry* **1971**, *10*, 1111−1120.
(11) Rothman, J. E.; Dawidowicz, E. A. Asymmetric Exchange of Vesicle Phospholipids Catalyzed by the Phosphatidylcholine Exchange Protein. Measurement of Inside−Outside Transitions. *Biochemistry* **1975**, *14*, 2809−2816.
(12) Johnson, L. W.; Hughes, M. E.; Zilversmit, D. B. Use of Phospholipid Exchange Protein to Measure Inside−Outside Transposition in Phosphatidylcholine Liposomes. *Biochim. Biophys. Acta, Biomembr.* **1975**, *375*, 176−185.
(13) Homan, R.; Pownall, H. J. Transbilayer diffusion of phospholipids: Dependence on headgroup structure and acyl chain length. *Biochim. Biophys. Acta, Biomembr.* **1988**, *938*, 155−166.
(14) Liu, J.; Conboy, J. C. 1,2-Diacyl-phosphatidylcholine flip-flop measured directly by sum-frequency vibrational spectroscopy. *Biophys. J.* **2005**, *89*, 2522−2532.
(15) Anglin, T. C.; Liu, J.; Conboy, J. C. Facile lipid flip-flop in a phospholipid bilayer induced by gramicidin a measured by sum-frequency vibrational spectroscopy. *Biophys. J.* **2007**, *92*, L01−L03.
(16) Anglin, T. C.; Conboy, J. C. Lateral pressure dependence of the phospholipid transmembrane diffusion rate in planar-supported lipid bilayers. *Biophys. J.* **2008**, *95*, 186−193.
(17) Anglin, T. C.; Cooper, M. P.; Li, H.; Chandler, K.; Conboy, J. C. Free energy and entropy of activation for phospholipid flip-flop in planar supported lipid bilayers. *J. Phys. Chem. B* **2010**, *114*, 1903−1914.
(18) Chan, Y.-H. M.; Boxer, S. G. Model membrane systems and their applications. *Curr. Opin. Chem. Biol.* **2007**, *11*, 581−587.
(19) Gerelli, Y.; Porcar, L.; Lombardi, L.; Fragneto, G. Lipid Exchange and Flip-Flop in Solid Supported Bilayers. *Langmuir* **2013**, *29*, 12762−12769.
(20) Heberle, F. A.; Marquardt, D.; Doktorova, M.; Geier, B.; Standaert, R. F.; Heftberger, P.; Kollmitzer, B.; Nickels, J. D.; Dick, R. A.; Feigenson, G. W.; Katsaras, J.; London, E.; Pabst, G. Subnanometer Structure of an Asymmetric Model Membrane: Interleaflet Coupling Influences Domain Properties. *Langmuir* **2016**, *32*, 5195−5200.
(21) Nakano, M.; Fukuda, M.; Kudo, T.; Matsuzaki, N.; Azuma, T.; Sekine, K.; Endo, H.; Handa, T. Flip-flop of phospholipids in vesicles: Kinetic analysis with time-resolved small-angle neutron scattering. *J. Phys. Chem. B* **2009**, *113*, 6745−6748.
(22) Kučerka, N.; Nagle, J. F.; Feller, S. E.; Balgavý, P. Models to analyze small-angle neutron scattering from unilamellar lipid vesicles. *Phys. Rev. E: Stat., Nonlinear, Soft Matter Phys.* **2004**, *69*, 051903.
(23) Kučerka, N.; Nieh, M.-P.; Katsaras, J. Fluid phase lipid areas and bilayer thicknesses of commonly used phosphatidylcholines as a function of temperature. *Biochim. Biophys. Acta, Biomembr.* **2011**, *1808*, 2761−2771.
(24) Mabrey, S.; Sturtevant, J. M. Investigation of phase transitions of lipids and lipid mixtures by sensitivity differential scanning calorimetry. *Proc. Natl. Acad. Sci. U.S.A.* **1976**, *73*, 3862−3866.
(25) Guard-Friar, D.; Chen, C. H.; Engle, A. S. Deuterium isotope effect on the stability of molecules: Phospholipids. *J. Phys. Chem.* **1985**, *89*, 1810−1813.
(26) Biltonen, R. L.; Lichtenberg, D. The use of differential scanning calorimetry as a tool to characterize liposome preparations. *Chem. Phys. Lipids* **1993**, *64*, 129−142.
(27) Katsaras, J.; Epand, R. F.; Epand, R. M. Absence of chiral domains in mixtures of dipalmitoylphosphatidylcholine molecules of opposite chirality. *Phys. Rev. E: Stat. Phys., Plasmas, Fluids, Relat. Interdiscip. Top.* **1997**, *55*, 3751−3753.
(28) Parente, R. A.; Lentz, B. R. Phase behavior of large unilamellar vesicles composed of synthetic phospholipids. *Biochemistry* **1984**, *23*, 2353−2362.
(29) Mason, P. C.; Gaulin, B. D.; Epand, R. M.; Wignall, G. D.; Lin, J. S. Small angle neutron scattering and calorimetric studies of large unilamellar vesicles of the phospholipid dipalmitoylphosphatidylcholine. *Phys. Rev. E: Stat. Phys., Plasmas, Fluids, Relat. Interdiscip. Top.* **1999**, *59*, 3361−3367.
(30) Heimburg, T. A Model for the Lipid Pretransition: Coupling of Ripple Formation with the Chain-Melting Transition. *Biophys. J.* **2000**, *78*, 1154−1165.
(31) Riske, K. A.; Barroso, R. P.; Vequi-Suplicy, C. C.; Germano, R.; Henriques, V. B.; Lamy, M. T. Lipid bilayer pre-transition as the beginning of the melting process. *Biochim. Biophys. Acta, Biomembr.* **2009**, *1788*, 954−963.
(32) Tamm, L. K.; McConnell, H. M. Supported Phospholipid Bilayers. *Biophys. J.* **1985**, *47*, 105−113.
(33) Czajkowsky, D. M.; Huang, C.; Shao, Z. Ripple phase in asymmetric unilamellar bilayers with saturated and unsaturated phospholipids. *Biochemistry* **1995**, *34*, 12501−12505.
(34) Fang, Y.; Yang, J. Role of the Bilayer−Bilayer Interaction on the Ripple Structure of Supported Bilayers in Solution. *J. Phys. Chem.* **1996**, *100*, 15614−15619.
(35) Kreutzberger, M. A.; Tejada, E.; Wang, Y.; Almeida, P. F. GUVs Melt Like LUVs: The Large Heat Capacity of MLVs is Not Due to Large Size or Small Curvature. *Biophys. J.* **2015**, *108*, 2619−2622.
(36) Perly, B.; Smith, I. C. P.; Hughes, L.; Burton, G. W.; Ingold, K. U. Estimation of the location of natural α-tocopherol in lipid bilayers by ^{13}C NMR spectroscopy. *Biochim. Biophys. Acta, Biomembr.* **1985**, *819*, 131−135.
(37) Bourdieu, L.; Silberzan, P.; Chatenay, D. Langmuir−Blodgett Films: From Micron to Angstrom. *Phys. Rev. Lett.* **1991**, *67*, 2029−2032.

DOI: 10.1021/acs.langmuir.6b04485
Langmuir 2017, 33, 3731−3741

(38) Mou, J.; Yang, J.; Shao, Z. Atomic Force Microscopy of Cholera Toxin B-Oligomers Bound to Bilayers of Biologically Relevant Lipids. *J. Mol. Biol.* **1995**, *248*, 507−512.
(39) Hui, S. W.; Viswanathan, R.; Zasadzinski, J. A.; Israelachvili, J. N. The structure and stability of phospholipid bilayers by atomic force microscopy. *Biophys. J.* **1995**, *68*, 171−178.
(40) Bassereau, P.; Pincet, F. Quantitative Analysis of Holes in Supported Bilayers Providing the Adsorption Energy of Surfactants on Solid Substrate. *Langmuir* **1997**, *13*, 7003−7007.
(41) Rinia, H. A.; Demel, R. A.; van der Eerden, J. P. J. M.; de Kruijff, B. Blistering of Langmuir−Blodgett Bilayers Containing Anionic Phospholipids as Observed by Atomic Force Microscopy. *Biophys. J.* **1999**, *77*, 1683−1693.
(42) Giocondi, M.-C.; Boichot, S.; Plénat, T.; Le Grimellec, C. Structural diversity of sphingomyelin microdomains. *Ultramicroscopy* **2004**, *100*, 135−143.
(43) Giocondi, M.-C.; Milhiet, P. E.; Dosset, P.; Le Grimellec, C. Use of Cyclodextrin for AFM Monitoring of Model Raft Formation. *Biophys. J.* **2004**, *86*, 861−869.
(44) Oliynyk, V.; Jäger, M.; Heimburg, T.; Buckin, V.; Kaatze, U. Lipid membrane domain formation and alamethicin aggregation studied by calorimetry, sound velocity measurements, and atomic force microscopy. *Biophys. Chem.* **2008**, *134*, 168−177.
(45) Giocondi, M.-C.; Yamamoto, D.; Lesniewska, E.; Milhiet, P.-E.; Ando, T.; Le Grimellec, C. Surface topography of membrane domains. *Biochim. Biophys. Acta, Biomembr.* **2010**, *1798*, 703−718.
(46) Wu, H.-L.; Tong, Y.; Peng, Q.; Li, N.; Ye, S. Phase transition behaviors of the supported DPPC bilayer investigated by sum frequency generation (SFG) vibrational spectroscopy and atomic force microscopy (AFM). *Phys. Chem. Chem. Phys.* **2016**, *18*, 1411−1421.
(47) Cheng, H.-T.; Megha; London, E. Preparation and Properties of Asymmetric Vesicles that Mimic Cell Membranes: Effect Upon Lipid Raft Formation and Transmembrane Helix Orientation. *J. Biol. Chem.* **2009**, *284*, 6079−6092.
(48) Son, M.; London, E. The dependence of lipid asymmetry upon phosphatidylcholine acyl chain structure. *J. Lipid Res.* **2013**, *54*, 223−231.
(49) Lin, Q.; London, E. Ordered Raft Domains Induced by Outer Leaflet Sphingomyelin in Cholesterol-Rich Asymmetric Vesicles. *Biophys. J.* **2015**, *108*, 2212−2222.
(50) Scomparin, C.; Lecuyer, S.; Ferreira, M.; Tinland, B. Diffusion in supported lipid bilayers: Influence of substrate and preparation technique on the internal dynamics. *Eur. Phys. J. E: Soft Matter Biol. Phys.* **2009**, *28*, 211−220.
(51) Sterling, S. M.; Dawes, R.; Allgeyer, E. S.; Ashworth, S. L.; Neivandt, D. J. Comparison of Actin- and Glass-Supported Phospholipid Bilayer Diffusion Coefficients. *Biophys. J.* **2015**, *108*, 1946−1953.
(52) Goksu, E. I.; Longo, M. L. Ternary Lipid Bilayers Containing Cholesterol in a High Curvature Silica Xerogel Environment. *Langmuir* **2010**, *26*, 8614−8624.
(53) Seeger, H. M.; Di Cerbo, A.; Alessandrini, A.; Facci, P. Supported Lipid Bilayers on Mica and Silicon Oxide: Comparison of the Main Phase Transition Behavior. *J. Phys. Chem. B* **2010**, *114*, 8926−8933.
(54) Crane, J. M.; Kiessling, V.; Tamm, L. K. Measuring Lipid Asymmetry in Planar Supported Bilayers by Fluorescence Interference Contrast Microscopy. *Langmuir* **2005**, *21*, 1377−1388.
(55) Kiessling, V.; Crane, J. M.; Tamm, L. K. Transbilayer Effects of Raft-Like Lipid Domains in Asymmetric Planar Bilayers Measured by Single Molecule Tracking. *Biophys. J.* **2006**, *91*, 3313−3326.
(56) Papahadjopoulos, D.; Jacobson, K.; Nir, S.; Isac, I. Phase transitions in phospholipid vesicles fluorescence polarization and permeability measurements concerning the effect of temperature and cholesterol. *Biochim. Biophys. Acta, Biomembr.* **1973**, *311*, 330−348.
(57) Nagle, J. F.; Scott, H. L. Lateral compressibility of lipid mono- and bilayers. Theory of membrane permeability. *Biochim. Biophys. Acta, Biomembr.* **1978**, *513*, 236−243.
(58) Cruzeiro-Hansson, L.; Mouritsen, O. G. Passive ion permeability of lipid membranes modelled via lipid-domain interfacial area. *Biochim. Biophys. Acta, Biomembr.* **1988**, *944*, 63−72.
(59) Liu, J.; Conboy, J. C. Phase transition of a single lipid bilayer measured by sum-frequency vibrational spectroscopy. *J. Am. Chem. Soc.* **2004**, *126*, 8894−8895.
(60) Kučerka, N.; Liu, Y.; Chu, N.; Petrache, H. I.; Tristram-Nagle, S.; Nagle, J. F. Structure of Fully Hydrated Fluid Phase DMPC and DLPC Lipid Bilayers Using X-ray Scattering from Oriented Multilamellar Arrays and from Unilamellar Vesicles. *Biophys. J.* **2005**, *88*, 2626−2637.
(61) Kučerka, N.; Pencer, J.; Sachs, J. N.; Nagle, J. F.; Katsaras, J. Curvature Effect on the Structure of Phospholipid Bilayers. *Langmuir* **2007**, *23*, 1292−1299.
(62) Brzustowicz, M. R.; Brunger, A. T. X-ray scattering from unilamellar lipid vesicles. *J. Appl. Crystallogr.* **2005**, *38*, 126−131.
(63) Chiantia, S.; Klymchenko, A. S.; London, E. A novel leaflet-selective fluorescence labeling technique reveals differences between inner and outer leaflets at high bilayer curvature. *Biochim. Biophys. Acta, Biomembr.* **2012**, *1818*, 1284−1290.
(64) Cheng, H.-T.; London, E. Preparation and Properties of Asymmetric Large Unilamellar Vesicles: Interleaflet Coupling in Asymmetric Vesicles is Dependent on Temperature but Not Curvature. *Biophys. J.* **2011**, *100*, 2671−2678.
(65) Chiantia, S.; Schwille, P.; Klymchenko, A. S.; London, E. Asymmetric GUVs Prepared by MβCD-Mediated Lipid Exchange: An FCS Study. *Biophys. J.* **2011**, *100*, L01−L03.
(66) Pautot, S.; Frisken, B. J.; Weitz, D. A. Engineering asymmetric vesicles. *Proc. Natl. Acad. Sci. U.S.A.* **2003**, *100*, 10718−10721.
(67) Okamoto, Y.; Motegi, T.; Morita, K.; Takagi, T.; Amii, H.; Kanamori, T.; Sonoyama, M.; Tero, R. Lateral Diffusion and Molecular Interaction in a Bilayer Membrane Consisting of Partially Fluorinated Phospholipids. *Langmuir* **2016**, *32*, 10712−10718.
(68) Jiang, F. Y.; Bouret, Y.; Kindt, J. T. Molecular dynamics simulations of the lipid bilayer edge. *Biophys. J.* **2004**, *87*, 182−192.
(69) Raphael, R. M.; Waugh, R. E.; Svetina, S.; Žekš, B. Fractional occurrence of defects in membranes and mechanically driven interleaflet phospholipid transport. *Phys. Rev. E: Stat., Nonlinear, Soft Matter Phys.* **2001**, *64*, 051913.
(70) Gurtovenko, A. A.; Vattulainen, I. Molecular Mechanism for Lipid Flip-Flops. *J. Phys. Chem. B* **2007**, *111*, 13554−13559.
(71) Heath, G. R.; Roth, J.; Connell, S. D.; Evans, S. D. Diffusion in low-dimensional lipid membranes. *Nano Lett.* **2014**, *14*, 5984−5988.
(72) Almeida, P. F. F. Thermodynamics of lipid interactions in complex bilayers. *Biochim. Biophys. Acta, Biomembr.* **2009**, *1788*, 72−85.
(73) Hill, W. G.; Rivers, R. L.; Zeidel, M. L. Role of leaflet asymmetry in the permeability of model biological membranes to protons, solutes, and gases. *J. Gen. Physiol.* **1999**, *114*, 405−414.
(74) Negrete, H. O.; Rivers, R. L.; Gough, A. H.; Colombini, M.; Zeidel, M. L. Individual Leaflets of a Membrane Bilayer Can Independently Regulate Permeability. *J. Biol. Chem.* **1996**, *271*, 11627−11630.
(75) Crane, J. M.; Tamm, L. K. Role of Cholesterol in the Formation and Nature of Lipid Rafts in Planar and Spherical Model Membranes. *Biophys. J.* **2004**, *86*, 2965−2979.
(76) Sackmann, E. Supported Membranes: Scientific and Practical Applications. *Science* **1996**, *271*, 43−48.
(77) Simons, K.; Gerl, M. J. Revitalizing membrane rafts: New tools and insights. *Nat. Rev. Mol. Cell Biol.* **2010**, *11*, 688−699.
(78) Wimley, W. C.; Thompson, T. E. Transbilayer and interbilayer phospholipid exchange in dimyristoylphosphatidylcholine/dimyristoylphosphatidylethanolamine large unilamellar vesicles. *Biochemistry* **1991**, *30*, 1702−1709.
(79) Dorairaj, S.; Allen, T. W. On the thermodynamic stability of a charged arginine side chain in a transmembrane helix. *Proc. Natl. Acad. Sci. U.S.A.* **2007**, *104*, 4943−4948.

DOI: 10.1021/acs.langmuir.6b04485
Langmuir 2017, 33, 3731−3741

(80) Tieleman, D. P.; Marrink, S.-J. Lipids out of equilibrium: Energetics of desorption and pore mediated flip-flop. *J. Am. Chem. Soc.* **2006**, *128*, 12462−12467.
(81) Sapay, N.; Bennett, W. F. D.; Tieleman, D. P. Thermodynamics of flip-flop and desorption for a systematic series of phosphatidylcholine lipids. *Soft Matter* **2009**, *5*, 3295.
(82) Lin, Q.; London, E. Preparation of artificial plasma membrane mimicking vesicles with lipid asymmetry. *PLoS One* **2014**, *9*, No. e87903.

DOI: 10.1021/acs.langmuir.6b04485
Langmuir 2017, 33, 3731−3741